ELSEVIER

Ultrasonic synthesis of polyaniline nanotubes containing Fe$_3$O$_4$ nanoparticles

Xiaofeng Lu[a], Hui Mao[a], Danming Chao[a], Wanjin Zhang[a],*, Yen Wei[b],**

[a]*Alan G. MacDiarmid Institute, Jilin University, Changchun 130012, PR China*
[b]*Department of Chemistry, Drexel University, PA 19104, USA*

Abstract

Polyaniline (PANI) nanotubes containing Fe$_3$O$_4$ nanoparticles were synthesized under ultrasonic irradiation of the aqueous solutions of aniline, ammonium peroxydisulfate (APS), phosphoric acid (H$_3$PO$_4$), and the quantitative amount of Fe$_3$O$_4$. It was found that the obtained samples had the morphologies of nanotubes. TEM images and selected area electronic diffractions showed that Fe$_3$O$_4$ nanoparticles were embedded in PANI nanotubes. We thought that the mechanism of the formation of PANI/Fe$_3$O$_4$ nanotubes could be attributed to the ultrasonic irradiation and the H$_3$PO$_4$–aniline salt template. The molecular structure of PANI/Fe$_3$O$_4$ nanotubes were characterized by Fourier transform infrared spectroscopy (FTIR), UV-vis absorption spectra and X-ray diffraction (XRD). The conductivity and magnetic properties of the PANI nanotubes containing Fe$_3$O$_4$ nanoparticles were also investigated.
© 2006 Elsevier Inc. All rights reserved.

Keywords: Polyaniline; Fe$_3$O$_4$; Ultrasonic irradiation; Nanotubes

1. Introduction

Since the discovery of carbon nanotubes by Iijima [1], one-dimensional (1D) nanostructures of various materials including metal, sulfide, metal oxides, polymer and even composite have been a subject of intense research because of their potential applications in many areas that include electronics, photonics, mechanics, and sensing [2–7]. On the other hand, polyaniline (PANI) is one of the most important conducting polymers because of its good processibility, environmental stability, and its oxidation- or protonation-adjustable electro-optical properties as well as its potential for a variety of applications [8–11]. In recent years, 1D nanostructures of PANI including nanowires, nanorods and nanotubes have been studied extensively. Many methods such as template method [12–14], template-free method [15,16] and even physical methods including electrospinning [17,18] and mechanical stretching [19] are used to prepare

1D nanostructures of PANI. Recently, interfacial polymerization, oligomer-assisted, nanofiber seeding and polymerization in dilute aniline aqueous solution method were also used to synthesize PANI nanofibers [20–23].

In addition, multifunctionalized PANI nanostructures have been prepared by blending PANI with inorganic electrical, optical, and magnetic nanoparticles to form nanocomposites [24,25]. Among the inorganic nanoparticles, Fe$_3$O$_4$ nanoparticles have received great attention because of their interesting magnetic properties as well as extensive potential applications in color imaging, magnetic recording media, soft magnetic materials and ferrofluids [26]. Recently, PANI/Fe$_3$O$_4$ nanocomposites have attracted more attention for applications of nanomaterials due to their novel properties. Wan et al. studied a series of PANI composites containing nanomagnets prepared by chemical polymerization [27]. Deng et al. reported the preparation of PANI-Fe$_3$O$_4$ nanoparticles with core-shell structure via an in situ polymerization of aniline monomer in an aqueous solution, which contains Fe$_3$O$_4$ nanoparticles and surfactant NaDS [28]. Few reports have studied the 1D nanostructures of PANI containing Fe$_3$O$_4$ nanoparticles. Wan et al. developed a self-assembly method to synthesize 1D PANI/Fe$_3$O$_4$

---

*Corresponding author. Fax: +86 431 5168924.
**Also to be correspondent.
E-mail addresses: xiaofeng@jlu.edu.cn (X. Lu), wjzhang@jlu.edu.cn (W. Zhang).

nanostructures, however, the content of Fe_3O_4 is little. High quantity nanotubes of PANI/Fe_3O_4 can be obtained when the Fe_3O_4/aniline mass ratio was lower [29]. Chan et al. prepared Y-junction PANI/Fe_3O_4 nanotubes. And the content of Fe_3O_4 nanoparticles was also only about 2.74 wt% [30]. So dispersing inorganic nanoparticles into PANI matrices is a meaningful object. Wang et al. developed a novel method to disperse TiO_2 and SiO_2 nanoparticles into PANI matrices under ultrasonic irradiation [31,32], and PANI/TiO_2 or PANI/SiO_2 composite nanoparticles can be obtained through this method. In our previous work, we reported an aniline dimer-COOH capped Fe_3O_4 nanoparticles assisting to synthesize PANI/Fe_3O_4 composite nanoparticles. Through this method, Fe_3O_4 nanoparticles could be dispersed in PANI matrices effectively, and high content Fe_3O_4 containing PANI/Fe_3O_4 composite nanoparticles were obtained [25].

In this paper, we reported a simple technique that allows the synthesis of PANI/Fe_3O_4 nanotubes by ultrasonic of aqueous solutions of aniline, ammonium peroxydisulfate (APS), phosphate acid, and the quantitative amount of aniline dimer-COOH capped Fe_3O_4 nanoparticles (Scheme 1). It was found that the obtained samples have the morphology of nanotubes. TEM images showed that Fe_3O_4 nanopaticles were embedded in PANI nanotubes. Moreover, when the content of Fe_3O_4 reached 20 wt%, high quantity nanotubes of PANI/Fe_3O_4 still can be prepared. To the best of our knowledge, this is the first example demonstrating the synthesis of 1D conducting polymers containing Fe_3O_4 nanoparticles under the ultrasonic irradiation.

2. Experimental

2.1. Materials

Aniline monomer was distilled under reduced pressure and stored below $0\,^{\circ}C$. All the other reagents were analytical grade, and used without further purification, including ammonium peroxydisulfate (APS), phosphoric acid (H_3PO_4), N-phenyl-1,4-phenylenediamine, succinic anhydride, diethyl ether, $FeCl_2 \cdot 4H_2O$, $FeCl_3 \cdot 6H_2O$, $NH_3 \cdot H_2O$, HCl, CH_2Cl_2 and methanol. Aniline dimer-COOH was synthesized by our group [25]. The reaction was carried out in a 100-mL three necked round bottom flask equipped with a mechanical stirrer, nitrogen inlet and outlet. N-phenyl-1,4-phenylenediamine 0.921 g (5.0 mmol) and succinic anhydride 0.500 g (5.0 mmol) were dissolved in 30 mL CH_2Cl_2 with stirring at room temperature for 5 h. As the reaction proceeded, white-grey precipitate was formed. At the end of reaction, the precipitate was collected by filtration and washed with diethyl ether until the filtrate became colorless. The product was dried under vacuum for 12 h at room temperature. Mass spectrum: 285.3 (MH^+/e). ^{1}H-NMR (500 MHz, DMSO) δ: 2.50 (s, 4H), 6.75(t, 1H), 7.00(dd, 4H), 7.18(t, 2H), 7.45(d, 2H), 8.02(s, 1H), 9.81(s, 1H), 12.13(s, 1H). A typical elemental analysis for $C_{16}H_{16}N_2O_3$: Found, C, 68.19, H, 5.95, N, 9.84, O, 17.10, Caled, C, 67.59, H, 5.67, N, 9.85, O, 16.88.

2.2. Synthesis of Fe_3O_4 nanoparticles

Fe_3O_4 nanoparticles were prepared based on our previous report [25]. $FeCl_2 \cdot 4H_2O$ (0.86 g) and $FeCl_3 \cdot 6H_2O$ (2.35 g) were dissolved under N_2 in deaerated Milli-Q water (20 mL) under vigorous stirring. As the solution was heated to 60 $^{\circ}C$, $NH_3 \cdot H_2O$ (28% (w/w), 5 mL) was added, quickly followed by addition of a solution of aniline dimer-COOH (200 mg) in 2 mL of acetone. The reaction was allowed to proceed for 1 h at 80 $^{\circ}C$ with constant and vigorous stirring to produce a stable, water-based suspension. The reaction mixture was then cooled slowly to room temperature. The suspension was washed sequentially with acetone and ethanol.

$$FeCl_2 \cdot 4H_2O \ + \ FeCl_3 \cdot 6H_2O \ + NH_3 \cdot H_2O + \ \text{aniline dimer-COOH} \longrightarrow$$
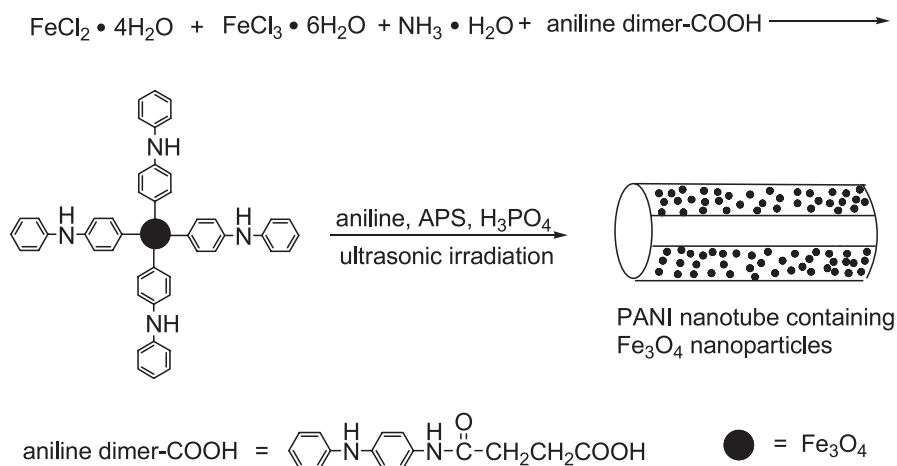
Scheme 1. Simplified schematic representation of the preparation of PANI/Fe_3O_4 composite nanotubes assisted by ultrasonic irradiation.

2.3. Preparation of PANI nanotubes containing Fe_3O_4 nanoparticles under ultrasonic irradiation

PANI nanotubes containing Fe_3O_4 nanoparticles were synthesized by ultrasonic irradiation method. In a typical procedure, 0.2 mL aniline monomer were mixed with H_3PO_4 (0.07 mL) and 10 or 20 wt% Fe_3O_4 dissolved in 15 mL of deionized water under ultrasonic stirring for 10 min to form an emulsion of aniline/H_3PO_4 complex containing Fe_3O_4 nanoparticles at room temperature. Then 5 mL aqueous solution of APS (0.46 g) was added to the above mixture. The reaction was kept by ultrasonic stirring for 4 h at the temperature between 25 and 30 °C. The resulting precipitate was washed with water and ethanol, respectively. Finally, the product was dried in vacuum at room temperature for 24 h.

2.4. Measurements

The ultrasonic experiments were carried out by an ultrasonic disperser (KQ 50 B, Kunshan ultrasonic Instrument Co. Ltd., 40 kHz, 50 W). Fourier transform infrared spectroscopy (FTIR) spectra of KBr powder-pressed pellets were recorded on a BRUKER VECTOR22 Spectrometer. Transmission spectra of PANI nanotubes containing different content of Fe_3O_4 nanoparticles by ultrasonic irradiation were recorded on a Shimadzu UV-3101 PC Spectrometer. X-ray diffraction patterns (XRD) were obtained with a Siemens D5005 diffractometer using Cu$K\alpha$ radiation. Scanning electron microscopy (SEM) measurements were performed on a SHIMADZU SSX-550 microscope. Transmission electron microscopy (TEM) experiments were performed on Hitachi H-8100 electron microscope with an acceleration voltage of 200 kV. ^{1}H-NMR spectra were run on a BRUKER-500 spectrometer, referenced to internal tetramethylsilane, with DMSO-d_6 as solvent. Mass spectroscopic studies were performed on an AXIMA CFR laser desorption ionization time of flight spectrometer (COMPACT). The standard Van Der Pauw DC four-probe method was used to measure the electron transport behavior of PANI nanotubes containing Fe_3O_4 nanoparticles. The samples of PANI/Fe_3O_4 were pressed into pellet. Then the pellet was cut into a square. The square was placed on the four-probe apparatus. Providing a voltage, a corresponding electrical current could be obtained. The electrical conductivity of samples was calculated by the following formular: σ (S/cm) $= (2.44 \times 10/S) \times (I/E)$, where σ is the conductivity; S is the sample side area; I is the current passed through outer probes; E is the voltage drop across inner probes. The room temperature magnetization in the applied magnetic field was performed by model JDM-13 vibrating sample magnetometer.

3. Results and discussion

The morphologies of the resulting PANI/Fe_3O_4 composites containing 10 and 20 wt% Fe_3O_4 are shown in Fig. 1.

SEM images reveal that both the samples have the morphologies of nanofibers. It seems that the diameter of the two samples are similar, and the length of PANI/Fe_3O_4 nanofibers containing 10 wt% Fe_3O_4 is a little longer than that of PANI/Fe_3O_4 samples containing 20 wt% Fe_3O_4. TEM images show that the PANI/Fe_3O_4 nanofibers are indeed nanotubes. From Fig. 2, we can find that the outer diameter of both samples is about 100 nm and the inter diameter is between 10 and 20 nm. TEM images also prove that the nanotubes consist of some small black particles. We believe that these particles are Fe_3O_4 nanoparticles, which can be further proved by electronic diffraction patterns. The index of each ring of the electronic diffraction patterns for Fe_3O_4 is in agreement with that of JCPDS (82-1533). Moreover, the electronic diffraction patterns indicate that the obtained Fe_3O_4 is crystalline. Compared to the composite samples containing 10 wt% Fe_3O_4 nanoparticles, there is a little aggregation of Fe_3O_4 nanoparticles in the composite nanotubes for the sample containing 20 wt% Fe_3O_4 nanoparticles. However, it provides a simple and effective method to synthesize
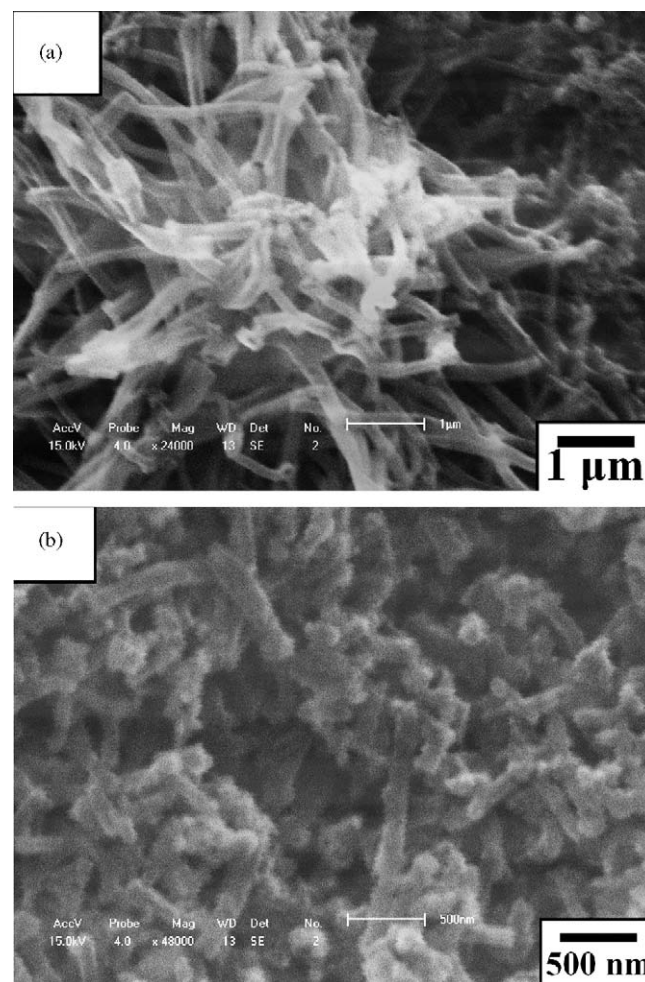

Fig. 1. SEM images of PANI nanotubes containing: (a) 10 wt% and (b) 20 wt% Fe_3O_4 nanoparticles by ultrasonic irradiation.

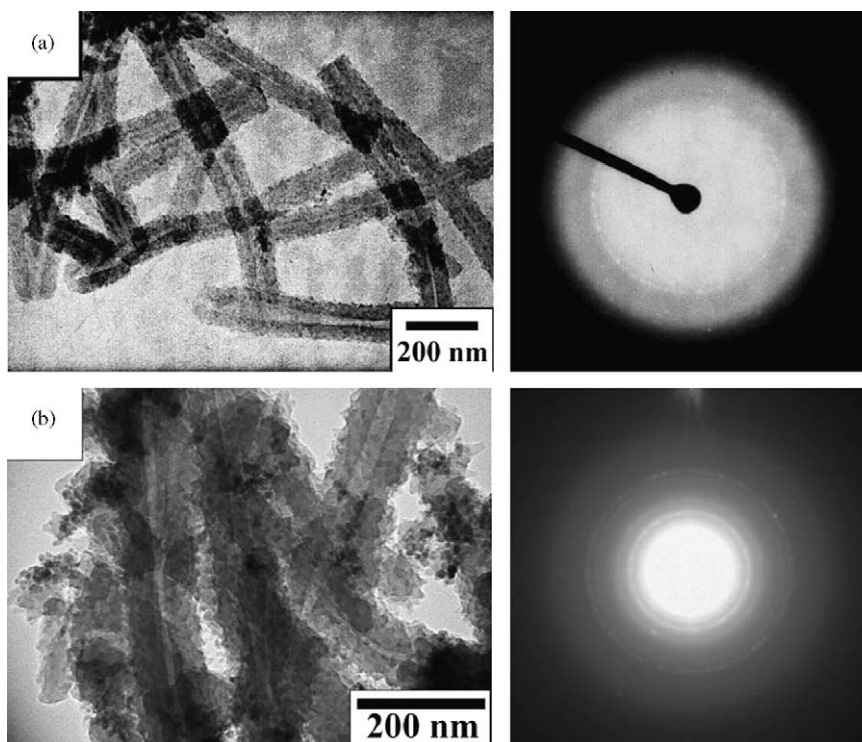Fig. 2. TEM images of PANI nanotubes containing: (a) 10 wt% and (b) 20 wt% Fe$_3$O$_4$ nanoparticles by ultrasonic irradiation. The right images show the selected area electronic diffractions of the PANI/Fe$_3$O$_4$ composite nanotubes.

PANI/Fe$_3$O$_4$ composite nanotubes containing relatively high content of Fe$_3$O$_4$ nanoparticles.

In an effort to elucidate the mechanism for the PANI/Fe$_3$O$_4$ nanotubes formation process, we polymerized the solution of aniline, APS, phosphate acid and 10 or 20 wt% Fe$_3$O$_4$ nanoparticles under magnetic stirring, it could only yield PANI/Fe$_3$O$_4$ power, no PANI/Fe$_3$O$_4$ nanotubes could be obtained. However, under the ultrasonic irradiation, PANI/Fe$_3$O$_4$ composite nanotubes could be observed. So we thought that it should be attributed to the ultrasonic irradiation. Huang et al. studied the mechanism of PANI nanofibers produced by interfacial polymerization and they thought that PANI preferentially forms as nanofibers in aqueous solution during chemical oxidative polymerization [33]. The nanofibers produced in the early stage of polymerization during slow-feeding reactions were subject to secondary growth, which led to the large agglomerates containing irregularly shaped particles. Pure nanofibers could be obtained by preventing the secondary growth. And in our method to synthesize PANI, the secondary growth was prevented effectively thanks to the ultrasonic irradiation, so the nanofibers could be obtained. As for the hollow fibers, besides the assistance of ultrasonic irradiation, the phosphate acid–aniline salt micelle might play an important role on the formation of the composite nanotubes [16,34]. In this reaction system, the concentration of the dopant (H$_3$PO$_4$) is low, the aniline is in excess. The dopant acid and its anilinium salt are expected to form

a special particle of micelles in the emulsion. Free aniline existing in the reaction solution might diffuse into the micelles to form micelles filled with free aniline that act as templates in the formation of PANI nanotubes. In order to prove this mechanism, we also prepared pure PANI sample in the same conditions. It was found that PANI nanotubes were obtained when the molar ratio of H$_3$PO$_4$ to aniline was lower than 1:2. However, when the molar ratio of H$_3$PO$_4$ to aniline is higher than 2:1, almost no tube-like PANI samples were observed (Fig. 3). This result was similar to Wan's report [16,34], which indicated the preferential templating effect. On the other hand, these nanotubes would highly aggregate and the number of granular nanoparticles formed under magnetic stirring at room temperature. Wan et al. prevented the aggregation under lower temperature (about 0 °C). Wang et al. reported that PANI could be well dispersed under ultrasonic irradiation [31,32]. In our experiments, the ultrasonic irradiation can prevent the aggregation of the nanotubes effectively, so the nanotubes were obtained. During the polymerization of PANI nanotubes, the aniline dimer-COOH capped Fe$_3$O$_4$ nanoparticles can be bonded to PANI nanotube matrices through graft polymerization, thus PANI/Fe$_3$O$_4$ composite nanotubes were synthesized.

FTIR spectra and XRD are used to characterize the molecular structures of PANI/Fe$_3$O$_4$ composite nanotubes. Fig. 4 shows the characteristic peaks of PANI/Fe$_3$O$_4$ composite nanotubes and PANI sample without Fe$_3$O$_4$
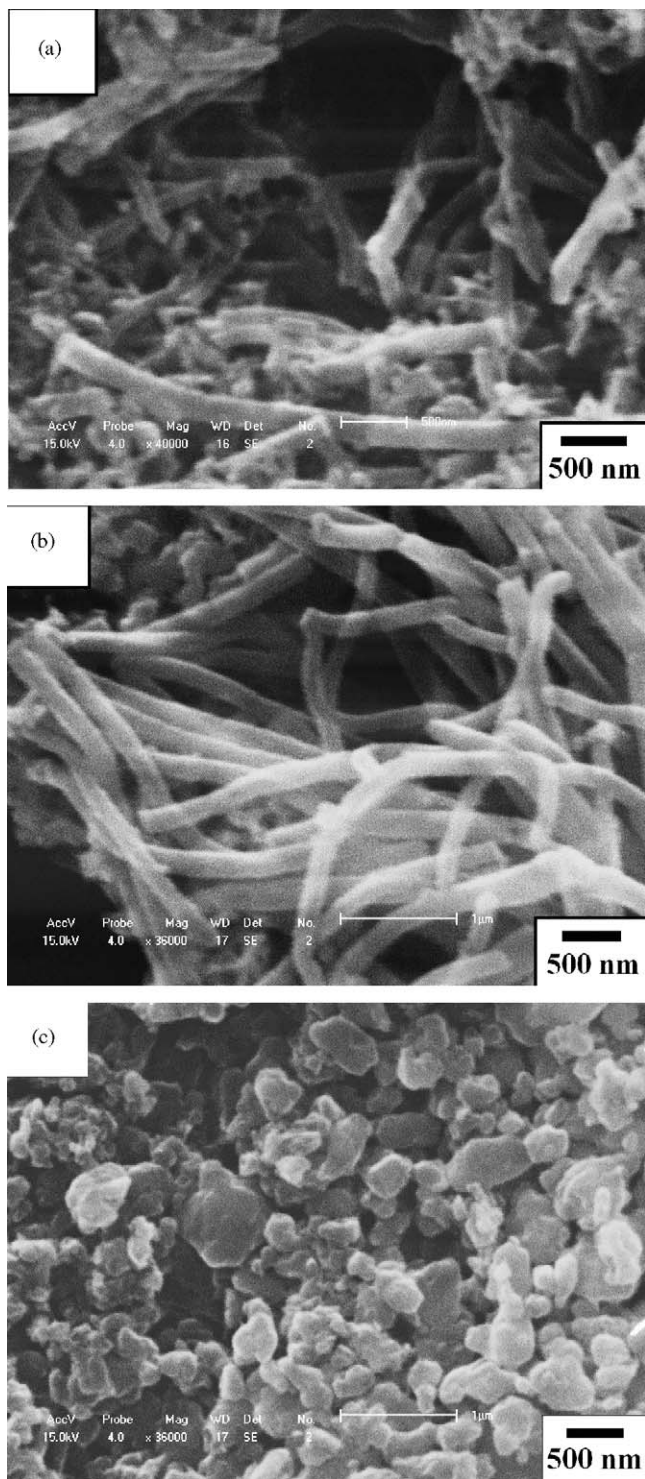
Fig. 3. SEM images of pure PANI nanotubes by ultrasonic irradiation under different molar ratio of H_3PO_4 to aniline: (a) H_3PO_4:aniline = 1:10; (b) H_3PO_4:aniline = 1:2; and (c) H_3PO_4:aniline = 2.5:1.

benzenoid ring, respectively), $1300\,cm^{-1}$ (C–N stretching of secondary aromatic amine), $1140\,cm^{-1}$, and $822\,cm^{-1}$ (out-of-plane deformation of C–H in the 1,4-disubstituted benzene ring), which is similar with that of PANI sample without Fe_3O_4 nanoparticles under the same conditions (Fig. 4a). All of these peaks are identical to those of PANI synthesized by a common method [35]. The XRD patterns of PANI/Fe_3O_4 composite nanotubes are shown in Fig. 5. The diffraction peaks of the Fe_3O_4 nanoparticles are observed in PANI/Fe_3O_4 nanotubes, including the peaks at $2\theta = 29.95°$, $35.45°$, $43.1°$, $57.25°$, and $62.8°$. These data are in good agreement with that of Fe_3O_4 synthesized in our previous report [25]. The broad peaks centered at $2\theta = 20°$ and $25°$ suggest that both the resulting PANI nanotubes are amorphous. Moreover, the two broad peaks (at about $21°$ and $25°$) can be ascribed to the periodicity
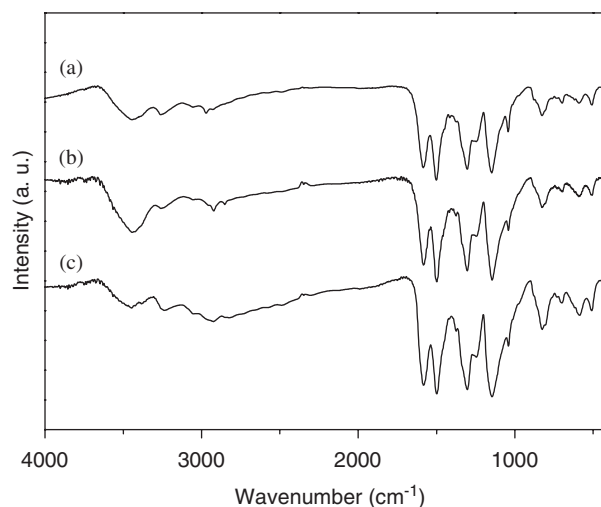

Fig. 4. FTIR spectra of PANI nanotubes containing: (a) 0 wt%, (b) 10 wt% and (c) 20 wt% Fe_3O_4 nanoparticles by ultrasonic irradiation.
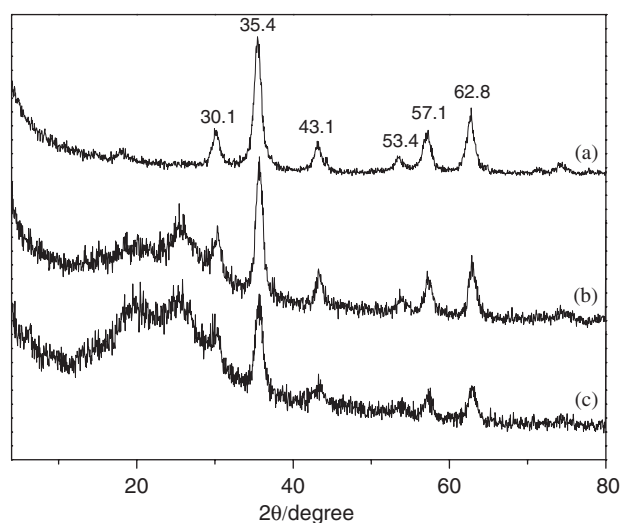

Fig. 5. XRD scattering patterns of: (a) aniline dimer-COOH capped Fe_3O_4 nanoparticles; (b) PANI nanotubes containing 20 wt% and (c) 10 wt% Fe_3O_4 nanoparticles by ultrasonic irradiation.

nanoparticles under the same conditions. It is found that PANI/Fe_3O_4 composite nanotubes have characteristic peaks at around $3234\,cm^{-1}$ (N–H stretching), $1582\,cm^{-1}$, $1493\,cm^{-1}$ (C=C stretching deformation of quinoid and

parallel and perpendicular to the polymer chain [36,37], respectively.

UV-vis spectra of the resulting $PANI/Fe_3O_4$ composite nanotubes dispersed in water were measured. In order to give a more careful assignation of UV-vis bands, we give the UV-vis spectra of pure PANI and $PANI/Fe_3O_4$ composite samples which were synthesized under ultrasonic irradiation (Fig. 6). It is found that the characteristic peaks of PANI at $\sim$280–340 (π–π* transition), $\sim$400–450 (polaron–π* transition), $\sim$780–900 nm (π–polaron transition) are observed. These results are consistent with previous Wang's report on $PANI/TiO_2$ composites and also proved the emeraldine salt form of PANI [31]. It is also found that with increased content of Fe_3O_4, the UV absorption of the π–polaron transition is shifted from 870 nm (0 wt% Fe_3O_4 nanoparticles content) to 830 nm (20 wt% Fe_3O_4 nanoparticles content). This result indicates that there is strong interaction between PANI and Fe_3O_4 nanoparticles. We also compare the UV-vis absorption spectra of the sample synthesized under ultrasound and conventional stirring method (Fig. 7). It is found that the UV-vis absorption at $\sim$280–340 nm is lower than that obtained through ultrasonic irradiation, which indicates that ultrasound improves the dispersion of Fe_3O_4 nanoparticles. This result is also consistent with that of $PANI/TiO_2$ system reported by Wang et al. in the literature [31].

The conductivities of the obtained $PANI/Fe_3O_4$ composite nanotubes are measured by the standard Van Der Pauw DC four-probe method. It is found that the conductivities of the $PANI/Fe_3O_4$ composite nanotubes containing 10 and 20 wt% Fe_3O_4 nanoparticles are similar and are 1.1×10^{-2} and 3.5×10^{-2} S/cm, respectively, which is a little lower than that of bulk PANI [35]. The lower conductivities of $PANI/Fe_3O_4$ composite nanotubes may be due to the lower concentration of dopant used in the polymerization process. The magnetic properties of the PANI nanotubes with Fe_3O_4 nanoparticles are investigated
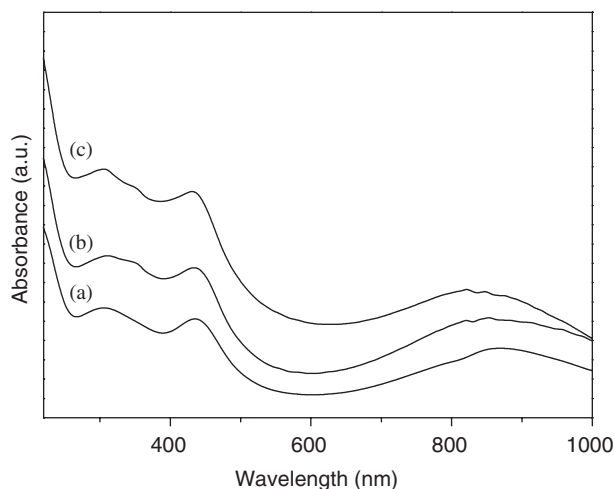

Fig. 6. UV/vis spectra of the obtained PANI nanotubes containing: (a) 0 wt% (b) 10 wt% and (c) 20 wt% Fe_3O_4 nanoparticles dispersed in water.
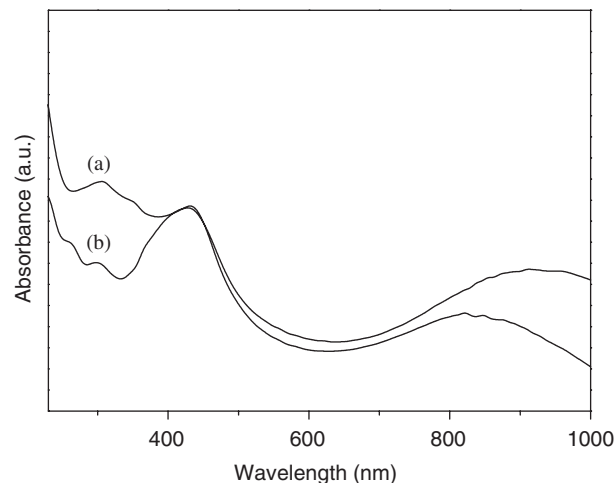

Fig. 7. UV/vis spectra of the obtained PANI samples containing 20 wt% Fe_3O_4 nanoparticles dispersed in water obtained through: (a) ultrasonic irradiation and (b) conventional stirring.
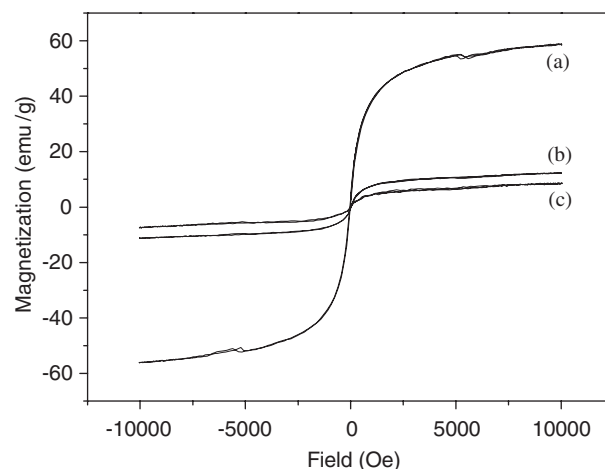

Fig. 8. Magnetization vs. applied magnetic field at room temperature for: (a) Fe_3O_4 nanoparticles and the PANI nanotubes containing (b) 20 wt% and (c) 10 wt% Fe_3O_4 nanoparticles by ultrasonic irradiation.

with a vibrating sample magnetometer. Typical magnetization curves as a function of applied field at room temperature (300 K) are shown in Fig. 8. There is no pronounced hysteresis loop, which indicates that both the retentivity and the coercivity of the composite nanotubes are zero. This observation is consistent with superparamagnetic behavior. As shown in Fig. 8, the $PANI/Fe_3O_4$ composite nanotubes have a saturated magnetization of $M_s = 8$ emu/g for the samples containing 10 wt% Fe_3O_4 nanoparticles and $M_s = 12$ emu/g for the samples containing 20 wt% Fe_3O_4 nanoparticles, which is a little lower than $PANI/Fe_3O_4$ nanocomposite with core-shell structure in our previous report [25].

4. Conclusions

In summary, we demonstrated a method to synthesize PANI nanotubes containing Fe_3O_4 nanoparticles under

ultrasonic irradiation of the aqueous solutions of aniline, APS, H_3PO_4, and the quantitative amount of aniline dimer-COOH capped Fe_3O_4 nanoparticles. TEM images showed the morphology of the composite nanotubes and also proved that Fe_3O_4 nanopaticles were embedded in the composites. FTIR, UV-vis absorption spectra and XRD characterized the molecular structure of PANI/Fe_3O_4 nanotubes. The conductivity and magnetic properties of the PANI nanotubes containing Fe_3O_4 nanoparticles showed that the samples have a novel conductivity and a superparamagnetic behavior.

Acknowledgements

References

[1] S. Iijima, Nature 354 (1991) 56.
[2] Y. Sun, Y. Xia, Adv. Mater. 14 (2002) 833.
[3] J. Yang, J.Y. Zeng, S.H. Yu, L. Yang, G. Zhou, Y.T. Qian, Chem. Mater. 12 (2000) 3259.
[4] P. Yang, H. Yan, S. Mao, R. Russo, J. Johnson, R. Saykally, N. Morris, J. Pham, R. He, H.J. Choi, Adv. Funct. Mater. 12 (2002) 323.
[5] J. Doshi, D.H. Reneker, J. Electrostat. 35 (1995) 151.
[6] Y. Zhang, K. Suenaga, S. Iijima, Science 281 (1998) 973.
[7] X. Lu, Y. Zhao, C. Wang, Adv. Mater. 17 (2005) 2485.
[8] A.G. MacDiarmid, J.C. Chiang, A.F. Richter, Synth. Met. 18 (1987) 285.
[9] Y. Cao, P. Smith, A.J. Heeger, Synth. Met. 48 (1992) 91.
[10] E.T. Kang, K.G. Neoh, K.L. Tan, Prog. Polym. Sci. 23 (1998) 277.
[11] P.F. Hutten, G. Hadziioannou, in: H.S. Nalwa (Ed.), Handbook of Organic Conducting Molecules and Polymers, vol. 3, Wiley, Chichester, 1997, p. 2.
[12] C.G. Wu, T. Bein, Science 264 (1994) 1757.
[13] R.V. Parthasarathy, C.R. Martin, Chem. Mater. 6 (1994) 1627.
[14] C.W. Wang, Z. Wang, M.K. Li, H.L. Li, Chem. Phys. Lett. 341 (2001) 431.
[15] H.J. Qiu, M.X. Wan, J. Polym. Sci. Part A: Polym. Chem. 39 (2001) 3485.
[16] Z.X. Wei, Z.M. Zhang, M.X. Wan, Langmuir 18 (2002) 917.
[17] D.H. Reneker, I. Chun, Nanotechnology 7 (1996) 216.
[18] A.G. MacDiarmid, W.E. Jones, I.D. Norns, J. Gao, A.T. Johnson, N.J. Pinto, J. Hone, B. Han, F.K. Ko, H. Okuzaki, M. Llaguno, Synth. Met. 119 (2001) 27.
[19] H.X. He, C.Z. Li, N.J. Tao, Appl. Phys. Lett. 78 (2001) 811.
[20] J. Huang, S. Virji, B.H. Weiller, R.B. Kaner, J. Am. Chem. Soc. 125 (2003) 314.
[21] W. Li, H.L. Wang, J. Am. Chem. Soc. 126 (2004) 2278.
[22] X. Zhang, W.J. Goux, S.K. Manohar, J. Am. Chem. Soc. 126 (2004) 4502.
[23] N.R. Chiou, A.J. Epstein, Adv. Mater. 17 (2005) 1679.
[24] X. Lu, Y. Yu, L. Chen, H. Mao, W. Zhang, Y. Wei, Chem. Commun. (2004) 1522.
[25] X. Lu, Y. Yu, L. Chen, H. Mao, H. Gao, J. Wang, W. Zhang, Y. Wei, Nanotechnology 16 (2005) 1660.
[26] J.L. Dormann, D. Fioranim, Magnetic Properties of Fine Particles, North-Holland, Amsterdam, 1991, pp. 309–423.
[27] M.X. Wan, W.C. Li, J. Polym. Sci. Part A: Polym. Chem. 34 (1997) 2129.
[28] J.G. Deng, C.L. He, Y.X. Peng, J.H. Wang, X.P. Long, P. Li, A.S.C. Chan, Synth. Met. 139 (2003) 295.
[29] Z.M. Zhang, M.X. Wan, Y. Wei, Nanotechnology 16 (2005) 2827.
[30] H. Xia, D. Chen, C. Xiao, H.S. Chan, J. Mater. Chem. 15 (2005) 2161.
[31] H. Xia, Q. Wang, Chem. Mater. 14 (2002) 2158.
[32] H. Xia, Q. Wang, J. Appl. Polym. Sci. 87 (2003) 1811.
[33] J.X. Huang, R.B. Kaner, Angew. Chem. Int. Ed. 43 (2004) 5817.
[34] Z.M. Zhang, Z.X. Wei, M.X. Wan, Macromolecules 35 (2002) 5937.
[35] G.E. Asturias, A.G. MacDiarmid, P.R. McCall, A.J. Epstein, Synth. Met. 29 (1989) E157.
[36] J.P. Pouget, M.E. J'ozefowicz, A.J. Epstein, X. Tang, A.G. MacDiarmid, Macromolecules 24 (1991) 77.
[37] Y.B. Moon, Y. Cao, P. Smith, A.J. Heeger, Polym. Commun. 30 (1989) 196.